

Optimization and finite element analysis of an in-wheel permanent magnet motor

Lassaad Zaaraoui*, Ali Mansouri*

Laboratory of Computer, Electronics & Smart Engineering Systems Design Engineering School of Sfax, B.P. W 3038, Sfax, Tunisia

* Corresponding authors: lassaad.zaaraoui@gmail.com (L. Zaaraoui), ali.mansouri@u-gafsa.tn (A. Mansouri)

Article history

Received 11 July 2020

Revised 28 January 2021

Accepted 1 February 2021

Abstract

Nowadays, artificial intelligence techniques have become widely used in electrical machines optimization and design. In this attempt, different methods have been proposed. The present work is devoted to the electromagnetic analysis and design of an in-wheel radial flux outer rotor surface mounted permanent magnet motor (SMPM) for electric vehicle application. Two based-Swarm Particle Optimization (PSO) techniques, namely, the improved PSO multi-Objective optimization and the Speed-constrained Multi-objective PSO Optimization, are applied. The main idea of the current optimization procedure is to determine the optimal machine sizing parameters providing the maximum of efficiency with the minimum of weight. To reach this goal, two objective functions are employed the efficiency maximization and the weight minimization. A preliminary analytical model describing the magnetic and electrical machine features was presented. In order to find the optimum design, the optimization results are discussed and analyzed. In addition, the electromagnetic performances of the found optimum design were studied by means of finite element analysis (FEA) and compared with those obtained by the optimization procedure.

Keywords: Multi-objective optimization, PSO-based techniques, permanent magnet machine, finite element analysis.

© 2021 Penerbit UTM Press. All rights reserved

INTRODUCTION

Recently, permanent magnet machines have become an attractive solution in many industrial applications such as electric and hybrid vehicle traction [1], [2] and wind power generation [3]. This is mainly due to their high efficiency, their compact structure, their small size, their low weight and their flexibility of control [1]. In order to achieve these features and to keep high airgap flux density, rare earth permanent magnets were used in these topologies. In the literature, several permanent magnet topologies were proposed. From these topologies, the most known are the radial flux machines, which are the most classic and the most emerged in industry, the axial flux machines and the transverse flux ones.

Lately, an original new machine design has become a promising solution for electric machines motoring. This design is called in-wheel motor in which the machine is directly placed interior the wheel hub [4], [5] and [6]. This technique enables the elimination of the gearbox difficulties involving low efficiency and common maintenance [7]. Generally, this motor consists of an outer rotor, fixed to the wheel and an inner stator. However, the machine can also be made up of inner rotor. In contrast of the inner rotor design, the outer rotor one is the most used in in-wheel electric vehicle applications [8] and [9]. This is due to that the large air gap diameter of the machine, allows a large number of poles, and because of the rotor is mounted on the machine outside, this topology is more appropriate for direct mounting in the wheel of the vehicle; which leads to a more compact system.

Furthermore, during operation, the permanent magnets will be subject of centrifugal forces; which make difficult their detachment.

Permanent magnet machines are characterized by a non-linear and complex magnetic circuit, making the optimal design a very difficult and time consuming task. For these reasons, an optimization tool is necessary. In the literature, several electric machines optimization techniques have been proposed.

In [10], the multi-objective genetic algorithm (GA) has been used to find the optimum design of a permanent magnet motor according to three objective functions. In [11], the optimal geometric parameters of an induction motor has been carried out by means of the GA. The same algorithm has been also used in [5] to determine the features of a permanent magnet machine with an outer rotor. In [12], a GA-based technique, for an electric machine design optimisation, has been introduced. Moreover, a nondominated sorting genetic algorithm II (NSGA-II) has been used in [13] to find the optimal design of a permanent magnet hub motor drive. The Particle Swarm Optimization (PSO) algorithm has been applied in [14] to optimize the dimensions and the performance of a permanent magnet motor. In the work presented in [15], the parametric estimation of an electric machine has carried out by applying the PSO algorithm. In order to minimize the losses in the magnets and to reduce the cogging torque, a PSO multi-objective optimization method has been introduced in [16]. The investigation of the optimum design of a permanent magnet motor with surface mounted magnets has been carried out by using also the PSO algorithm [17].

Based on this brief study, we can conclude that the use of multi-objective optimization techniques has become an increasing and a powerful tool in electrical machines design.

As mentioned, several problems are encountered when modeling the electromagnetic fields in electrical machine. The magnetic saturation, the non-linearity of the materials and the anisotropic behavior of the laminated parts of the iron core, makes the analytical modeling a challenging task. Nowadays, a best way to model electrical machines is to use the finite element analysis (FEA) tool.

The present work aims to the optimum design of an outer rotor concentrated windings permanent magnet motor. A preliminary analytical machine model is firstly presented and then used in the optimization procedure. Two PSO-based multi-objective optimization techniques are used. In order to find the optimum machine design, the obtained Pareto fronts are analyzed and discussed. Finally, the machine performances are investigated by means of FEA.

USED ARTIFICIAL INTELLIGENT TECHNIQUES

As it was mentioned, two PSO-based techniques are used for machine optimization. These techniques are described in the following.

OMOPSO algorithm

An improved Particle Swarm Optimization algorithm has been introduced in [18]. This optimization technique is based on the Pareto dominance. In order to filter out the list of available leaders, a crowding factor is applied. Therefore, the swarm is divided into three sub-swarms with the same size. Then, a different mutation technique is applied in each sub-swarm. This mutation technique is applied in order to enhance the the swarm diversity. From the set of existing leaders, the leader is arbitrarily selected with probability Ps. All of leaders are stored in an external archive. The update of this archive is based on the crowding factor.

Speed-constrained Multi-objective PSO (SMPSO)

Another PSO-based optimization technique has been proposed in [19]. This technique aims to enhance the research capacity and to limit the velocity of the particle in the OMOPSO algorithm. When the speed is very high, the SMPSO algorithm allows the generation of new efficient particle’s locations. In order to preserve the non-dominated solutions found during the search process, the SMPSO algorithm uses an external archive, and as a turbulence factor this algorithm use of polynomial mutation [19].

STUDIED MACHINE DATA

In this work, the studied topology is a synchronous, 3-phase, 18-pole, 26 kW and 27-slots permanent magnet motor with surface mounted magnets. In this machine the rotor is mounted on the outside. The stator consists of a laminated iron core and a three phase concentrated windings. The rotor is made up of alternating magnetized permanent magnets mounted and an iron core. The magnets, radially magnetized, produces a magnetic field. The major machine features and geometric dimensions are respectively illustrated in Fig. 1.

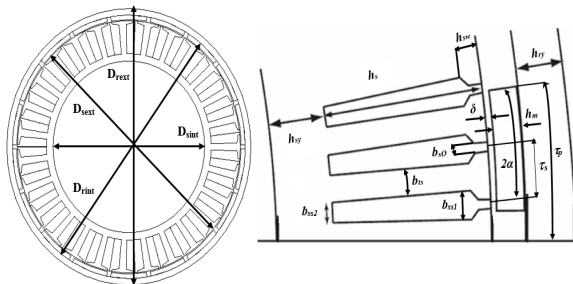


Fig. 1 Machine features and geometric dimensions

PRELIMINARY ANALYTICAL MODEL

In all machine design procedures, the use of an appropriate analytical model is a crucial task. Owing to this model, we can

estimate and compare the machine features by detmrining the output torque, the machine losses and efficiency.

This section aims to the presentation of the analytical model describing both magnetic and electric properties of the studied machine.

The main sizing dimensions of the considered topology are shown in Fig. 1. The relations dealing with these dimensions are presented in the following equations. This model was described in a previos work [23].

Machine sizing

Slot pitch τ_s :

$$\tau_s = \pi \frac{D_{sext}}{Q_s} \tag{1}$$

Q_s is number of stator slots and D_{sext} is the stator outer diameter.

Pole pitch τ_p :

$$\tau_p = \pi \frac{D_{sext}}{2p} \tag{2}$$

p is the pole pairs number.

Width of the inner stator slot b_{ss1} :

$$b_{ss1} = \pi \frac{D_{sext} - 2h_{sw}}{Q_s} - b_{ts} \tag{3}$$

b_{ts} is the width of the stator tooth and h_{sw} is the height of the slot wedge.

Width of the outer stator slot b_{ss2} :

$$b_{ss2} = \pi \frac{D_{sext} - 2h_s}{Q_s} - b_{ts} \tag{4}$$

h_s is the stator slot height.

Opening factor of the slot k_{open} :

$$k_{open} = \frac{b_{ss0}}{b_{ss1}} \tag{5}$$

b_{ss0} is the opening of the stator slot.

Height of the stator yoke h_{sy} :

$$h_{sy} = \frac{1}{2}(D_{sext} - D_{sint} - 2h_s) \tag{6}$$

D_{sint} is the inner diameter of the stator.

Outer diameter of the stator D_{sext} :

$$D_{sext} = D_{rint} - 2h_m - 2\delta \tag{7}$$

δ , D_{rint} , h_m and are respectively the length of the airgap, the inner diameter of the rotor and the height of the magnet.

Height of the rotor yoke h_{ry} :

$$h_{ry} = \frac{1}{2}(D_{rext} - D_{rint}) \tag{8}$$

D_{rint} is the inner diameter of the rotor.

Magnetic modelling

The magnetic flux densities in the airgap, in the stator tooth, in the stator yoke and in the rotor yoke are outlined.

Airgap flux density

When optimizing an electrical machine, the fundamental airgap flux density amplitude is a crucial parameter. In radially magnetized

magnets, the maximum value of the airgap flux density, (B_m), produced by the magnets is given by [9]:

$$B_m = \frac{h_m}{h_m + \mu_r \delta_c} B_r \tag{9}$$

B_r is the magnet remanence flux density and μ_r is its relative permeability. δ_c is the length of the effective airgap, defined from the cart's, k_c , coefficient by:

$$\delta_c = k_c \delta \tag{10}$$

k_c is given by the following equation [9]:

$$k_c = \frac{\tau_s}{\tau_s - \frac{(b_{ss0}/\delta)^2}{5 + b_{ss0}/\delta} \delta} \tag{11}$$

The amplitude of the fundamental of flux density in the airgap, B_g , is then expressed as [20] and [21]:

$$B_g = \frac{4}{\pi} B_m \sin(\alpha) \tag{12}$$

Where 2α (electric angle) is the pole angle arc, given by [9]:

$$\alpha = \frac{\pi w_m}{2 \tau_p} \tag{13}$$

Where w_m is the pole width and τ_p is the pole pitch.

Flux densities in the machine iron regions

The machine iron regions are the stator yoke, the stator teeth and the rotor yoke. In these regions, the flux densities are respectively, B_{sy} , B_{st} , and B_{ry} . These flux densities are expressed as follows [3] and [9]:

$$B_{sy} = \frac{\tau_p B_g}{2h_{sy}} \tag{14}$$

$$B_{st} = \frac{\tau_p B_g 2p}{b_{ts} Q_s} \tag{15}$$

$$B_{ry} = \frac{\tau_m B_m}{2h_{ry}} \tag{16}$$

Electric modelling

In the following, the electric features of the studied machine are presented.

Electromotive force

Neglecting the flux leakage, the fundamental of the electromotive force in phase a ($\hat{E}_{a,1}$), can be determined by [3] and [9]:

$$\hat{E}_{a,1} = \pi \sqrt{2} f N_c B_g k_{w1} \frac{D_{sext} l}{p} \tag{17}$$

Where f is the electrical frequency, N_c is the number of a phase winding turns, k_{w1} is the fill factor and l is the effective machine length.

Electromagnetic power

In a three-phase permanent magnet machine, the root mean square (rms) electromagnetic power, P_{em} , is calculated according to the following equation:

$$P_{em} = 3 \hat{E}_{a,1} \hat{I}_s \sin \beta \tag{18}$$

Where \hat{I}_s the current amplitude and β is the electrical angle between the magnet flux and the current.

Electromagnetic torque

For electric drives, the electromagnetic torque is provided by dividing the electromagnetic power by the speed of the rotor.

$$T_{em} = \frac{3}{\sqrt{2}} N_c B_g k_{w1} D_{sext} l \hat{I}_s \sin \beta \tag{19}$$

For the considered machine in the current survey, the rms torque T_{rms} is expressed from the the peak value of the fundamental current loading \hat{S}_1 and it is given by the following equation [22]:

$$T_{rms} = \frac{\pi}{4} \hat{B}_g \hat{S}_1 D_{sext}^2 l \sin \beta \tag{20}$$

Copper loss

In an electrical machines, the copper loss, P_{cu} , is due to current flowing through the stator windings. It is determined from the winding resistance of a phase, R_{ph} , and the square of the phase current, I_{ph} . Copper loss in [W], is calculated as [23]:

$$P_{cu} = 3 R_{ph} I_{ph}^2 \tag{21}$$

Iron losses

Three iron losses components named, static hysteresis losses P_h , classical eddy currents losses P_c and excess losses P_e , can be distinguished [23]. In the frequency domain and supposing that the flux density is sinusoidal, the iron losses in the stator teeth P_{st} , in the stator yoke P_{sy} , and in the rotor yoke P_{ry} , are estimated by applying the following model [1], [20] and [23]:

$$P_{st} = \left(k_h f B_{st}^\beta + \pi^2 \frac{\sigma d^2}{6} B_{st}^2 f^2 + 8.67 k_c f^{1.5} B_{st}^{1.5} \right) V_{st} \tag{22}$$

$$P_{sy} = \left(k_h f B_{sy}^\beta + \pi^2 \frac{\sigma d^2}{6} B_{sy}^2 f^2 + 8.67 k_c f^{1.5} B_{sy}^{1.5} \right) V_{sy} \tag{23}$$

$$P_{ry} = \left(k_h f B_{ry}^\beta + \pi^2 \frac{\sigma d^2}{6} B_{ry}^2 f^2 + 8.67 k_c f^{1.5} B_{ry}^{1.5} \right) V_{ry} \tag{24}$$

V_{st} , V_{sy} , k_h , V_{ry} are the volumes of the stator teeth, the stator and the rotor yokes. σ , d , k_c , k_h , and β are respectively the conductivity and the thickness of the iron lamination, the eddy current and the hysteresis coefficients and the Steinmetz constant.

OPTIMIZATION RESULTS

In order to determine the geometric parameters of the studied machine, a PSO-based multi-objective optimization procedure is carried out. The efficiency maximization and the weight minimization are used as objective functions.

$$objective_function1 = minimum(1 - \eta) \tag{25}$$

Where η is machine efficiency calculated by:

$$\eta = \frac{P_{out}}{P_{out} + P_{cu} + P_{st} + P_{sy} + P_{ry}} \tag{26}$$

$$objective_function2 = minimum(weight) \tag{27}$$

Weight function is the machine weight.

Design Variables

In the present work, the sizing parameters are: the inner diameter of the rotor D_{rint} , the height of the magnets h_m , the length of the airgap δ , the height of the slot wedge h_{sw} , the height of the stator slot h_s , the width of the stator teeth b_{ts} , the angle of the magnet α , the machine active length l and the inner diameter of the stator D_{sint} .

Constraints

In order to avoid the magnetic saturation and to ensure the mechanical rigidity of the structure, a set of constraints is added to the optimization problem. The used constraints are given Table 1.

Table 1 Optimization problem constraints [23].

	Variables	Constraints
Mechanical constraints	h_{sw}	$h_{sw} \geq 2$
	b_{ts}	$b_{ts} \geq 0.3\tau_s$
	b_{ss2}	$0.15h_{ss} \leq b_{ss2} \leq 0.5h_{ss}$
Magnetic constraints	B_{st}	$B_{st} \leq 2$
	B_{sy}	$B_{sy} \leq 1.8$
	B_{ry}	$B_{ry} \leq 1.8$
	B_g	$B_g \leq 1.05$

Once the optimization problem is defined, the optimization procedure is conducted by the implementation of the OMOPSO and the SMPSO algorithms. As results, we are interested to the Pareto fronts and the optimization output. The first ones corresponding respectively to the OMOPSO and SMPSO algorithms are illustrated in Fig. 2 and Fig.3. The final output optimization results are reported in Table 2.

Table 2 Optimization results

Parameter	OMOPSO	SMPSO
δ (mm)	1.6	1.6
D_{rint} (mm)	286	286
h_m (mm)	3	3
h_{sw} (mm)	2	2
b_{ts} (mm)	15	15
h_s (mm)	35	35
l (mm)	50	50
α (°)	16	16
D_{sint} (mm)	183.2	183.4
Efficiency (%)	0,981	0,985
weight (kg)	31,44	32,55
CPU (s)	18.256	12.549

Since all of Pareto front values, shown in Fig. 2, are feasible, the designer has to choose, from the Pareto fronts, the suitable parameters satisfying the specific design requirements. We can notice in Fig. 2 that both of SMPSO and OMOPSO techniques provide an optimal Pareto front concerning the considered optimization problem. Moreover, we can also clearly remark, the contradiction in the machine weight and efficiency variations. Thus, an increase in the machine produces an increase of the machine weight. One further comment that we can mention, is that the SMPSO algorithm is slightly faster than the OMOPSO one.

FEA RESULTS

With the final aim of confirming the performance and efficiency of the optimization techniques, the machine model was validated by deep finite element simulations. Because of the the symmetry and the periodicities in the studied topology, the FEA investigations were reduced to the machine ninth. The FEA results are illustrated in Fig. 4, Fig. 5 and Table 3.

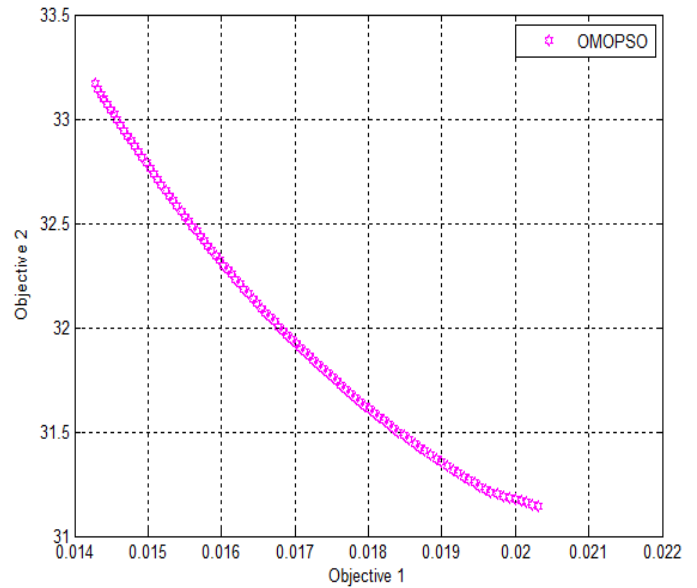


Fig. 2 OMOPSO Pareto front

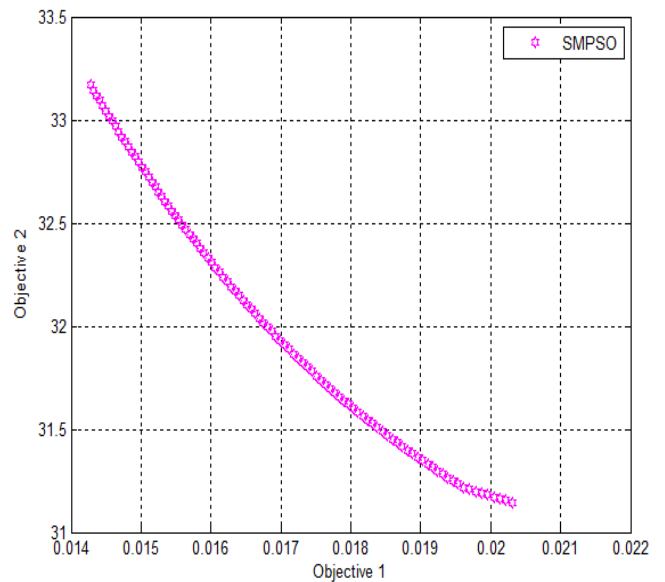


Fig. 3 SMPSO Pareto front

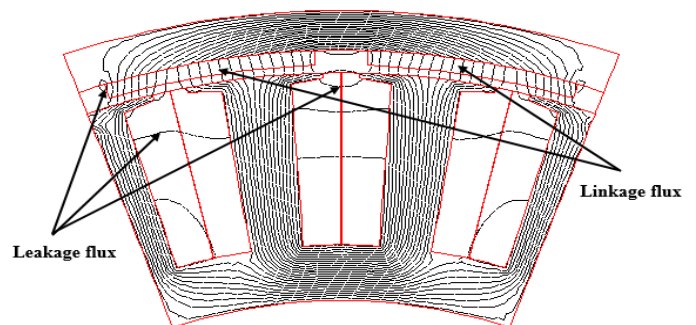


Fig. 4 Plot of 2-D flux lines

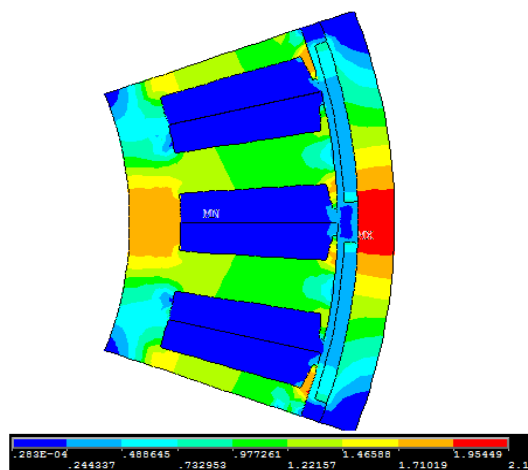


Fig. 5 Distribution of the magnetic Flux density

Table 3 Comparison between Optimization and FEA results

Parameter	Optimization results	FEA results	Error (%)
B_m (T)	0.72	0.72	0
B_g (T)	0.88	0.91	3.3
B_{sy} (T)	1.79	1.77	1.1
B_{st} (T)	1.75	1.85	5.4
B_{ry} (T)	1.86	2.1	7.5
Total Iron losses (kW)	1.057	1.064	0.7

Referring to Fig. 4, we can notice the existence of flux lines which do not cross the airgap. These flux lines are the leakage flux.

The flux density distributions of the studied machine, from 2-D FEA results, are shown in Fig. 5. It can be clearly noticed that some saturations occur in the rotor iron core and some small areas in the stator teeth.

DISCUSSION

After several executions, the OMOPSO and SMPSO algorithms show that they can overcome the problem of the contradictions of the objective functions, since the maximization of the machine efficiency causes a maximization of its weight and vice versa. Indeed, these two algorithms are capable of generating optimal solutions which satisfy all the objective functions and the imposed constraints. Moreover, the figures of the Pareto fronts show that the algorithms make it possible to generate fronts rich with non-dominated solutions, and that they do not quickly lose their diversity. Furthermore, the simulations results of the electromagnetic features, which are calculated by means of finite element analysis (FEA), show a good agreement with the algorithms results.

CONCLUSION

This work is devoted to the optimal sizing of an in-wheel, outer rotor, surface mounted permanent magnet motor. To achieve this, two based-Swarm Particle Optimization (PSO) techniques, namely, the improved PSO multi-Objective optimization and the Speed-constrained multi-objective PSO (SMPSO) optimization, were implemented. The target of our optimization procedure is to find the optimum machine's geometric parameters leading to the maximum efficiency and the minimum weight. Based on the obtained Pareto fronts, from the multi-objective optimization procedure, a topology is selected. In order to confirm the analytical optimization, the selected topology was analyzed by FEA. Simulation results of FEA illustrated that the results obtained by analytical optimization are in good agreement with those obtained by FEA.

REFERENCES

[1] Zhu ZQ, Howe D. Electrical machines and drives for electric, hybrid and fuel cell vehicles. P IEEE 2007; 95: 746–765.

[2] Wang J, Atallah K, Zhu ZQ, Howe D. Modular 3-phase permanent magnet brushless machines for in-wheel applications. IEEE T Veh Technol 2008; 57: 2714–720.

[3] Strous TD. Design of a permanent magnet radial flux concentrated coil generator for a range extender application. MSc, Delft University of Technology, Netherlands, 2010.

[4] Chan CC, Chau KT. Modern electric vehicle technology. New York, USA: Oxford University Press, 2001.

[5] Wrobel R, Mellor P. Design considerations of a direct drive brushless machine with concentrated windings. IEEE T Energy Conver 2008; 23: 1-8.

[6] Rix A, Kamper M, Wang R. Design and performance evaluation of concentrated coil permanent magnet machines for in-wheel drives. In: IEEE 2007 International Electric Machines and Drives Conference; 3-5 May 2007; Antalya, Turkey.

[7] Andriollo M, Bettanini G, Martinelli G, Morini A, Stellin S, Tortella A. In-wheel permanent magnet motors for public transport application. In: 5th 2005 International Conference on Electric Power Systems, High Voltages, Electric Machines; 16-18 December 2005; Tenerife, Canary Islands, Spain.

[8] Wu D, Fei W, Luk PCK, Xia B. Design considerations of outer-rotor permanent magnet synchronous machines for in-wheel electric vehicle applications using particle swarm optimization. In: IET 2014 7th International Conference on Power Electronics, Machines and Drives; 8-10 April 2014; Manchester, United Kingdom.

[9] Hung VX. Modelling of exterior rotor permanent magnet machines with concentrated windings, MSc, Faculty of Electrical Engineering, Mathematics and Computer Science, Netherlands, 2012.

[10] Markovic M, Ragot P, Perriard Y. Design optimization of a BLDC motor: a comparative analysis. In: IEEE 2007 International Electric Machines and Drives Conference; 3-5 May 2007; Antalya, Turkey.

[11] Ilka R, Tilaki A R, Alamdari HA, Baghipour R. Design optimization of permanent magnet-brushless DC motor using elitist genetic algorithm with minimum loss and maximum power density. Int J Mechatron Electr Comput Technol. 2014; 4: 1169-1185.

[12] Ahn Y, Park J, CG Lee, Kim JW, and Jung SY. Novel memetic algorithm implemented with GA (Genetic Algorithm) and MADS (Mesh Adaptive Direct Search) for optimal design of electromagnetic system. IEEE T Magn 2010; 46: 1982-1996.

[13] Sun X, Cai Y. Driving-Cycle Oriented design optimization of a permanent magnet hub motor drive system for a four-wheel-drive electric vehicle. IEEE Transactions on Transportation Electrification, 2020, 6: 1115-1125.

[14] Izanlo A, Gholamian S. A, Abdollahi S. E. Optimal design of a permanent magnet synchronous motor for high efficiency and low cogging torque. International Journal on Electrical Engineering and Informatics, 2020, 12: 173-186.

[15] Sakthivel VP, Bhuvanewari R, Subramanian S. Multi-objective parameter estimation of induction motor using particle swarm optimization. Eng Appl Artif Intel 2010; 23: 302–312.

[16] Ashabani M, Rady YA, Mohamed I. Multi-objective shape optimization of segmented pole permanent-magnet synchronous machines with improved torque characteristics. IEEE T Magn 2011; 47: 795-804.

[17] Mutluer M, and Bilgin O. Design optimization of PMSM by particle swarm optimization and genetic algorithm. In: IEEE 2012 International Symposium on Innovations in Intelligent Systems and Applications; 2-4 July 2012; Trabzon, Turkey.

[18] Sierra MR, Coello C. Improving PSO-based multi-objective optimization using crowding, mutation and e – dominance. In: 2005 Third International Conference on Evolutionary Multi-Criterion Optimization; 9-11 March 2005; Guanajuato, Mexico

[19] Nebro AJ, Durillo JJ, Nieto JG, CAC, Luna F, Alba E. SMPSO: A new PSO-based metaheuristic for multi-objective optimization. In: IEEE 2009 Symposium on Computational Intelligence in Multi-criteria Decision-Making; 30 March-02 April 2009; Nashville, TN, USA.

[20] Mansouri A, Msaddek H, Trabelsi H. Optimum Design of a surface mounted fractional slots permanent magnet motor. Int Rev Electr Eng 2015; 10: 28-35.

[21] Feng Y. L, Zhang C. N. Analytical calculation for predicting the air gap flux density in surface-mounted permanent magnet synchronous machine. Journal of Electrical Engineering and Technology, 2017; 12: 769-777.

[22] Bianchi N, Bolognani S. Design criteria of high efficiency SPM synchronous motors. IEEE T Energy Conver 2006; 21: 396-404.

[23] Mansouri A, Smairi N, Trabelsi H. Multi-objective optimization of an in-wheel electric vehicle motor. Int J Appl Electromagn Mech, 2016; 50: 449-465.